

Final Technical Report

USGS NEHRP Award G11AP20062

Evaluating the potential for long-term strain accumulation down-dip of the locked zone
by quantifying the release of strain from slow slip on the Cascadia subduction zone

David Schmidt (das@uoregon.edu*)
Ray Weldon (ray@uoregon.edu)
Randy Krogstad (krogstad@uoregon.edu)

Department of Geological Sciences
University of Oregon
1272 University of Oregon
Eugene, OR 97403-1272
Fax: 541-346-4692

* New contact info: dasc @ uw.edu, 206-685-3799

Award Period: March 2011 through March 2012

Research supported by the U.S. Geological Survey (USGS), Department of the Interior, under USGS award number G11AP20062. The views and conclusions contained in this document are those of the authors and should not be interpreted as necessarily representing the official policies, either expressed or implied, of the U.S. Government.

Abstract

Most interseismic locking models for the Cascadia subduction zone predict that the long-term strain accumulation rate decreases in a linear or exponential fashion from the shallow locked zone to the deep extension of the plate interface that slides freely. Slow slip events and non-volcanic tremor map to the base of this transition zone where it is inferred minimal strain accumulates. However, strain does accumulate in this region over short periods (on the order of months) before it is released by slow slip and tremor. Here we explore whether strain can also be stored over the long-term (decadal time periods) in the region of slow slip and tremor. We modeled the uplift rates from leveling data spanning approximately 80 years in Washington and Oregon using elastic dislocation models. We find that the leveling data can be best fit with models that include long term locking up to 20% of the plate-rate near the updip edge of the ETS zone. This accumulated strain could be released in future slow slip events, as afterslip, or during a future megathrust event. If the strain is released seismically, then it would extend the seismogenic zone closer to urban populations than previously appreciated.

Introduction

Episodic tremor and slow slip (ETS) events represent the transient release of accumulated strain along the plate interface at 25-45 km depth, and occur downdip from the seismogenically locked zone. The $\sim M_w$ 6 ETS events in Cascadia last approximately 10-20 days and have recurrence intervals of 11-22 months [Dragert *et al.*, 2001; Rogers and Dragert, 2003; Schmidt and Gao, 2010]. The existence of ETS demonstrates that the plate interface is capable of storing strain at this depth, if only for months or years. The limited resolution of slip on the plate interface leaves some uncertainty as to whether any permanent strain might accumulate over multiple ETS cycles, thereby potentially elevating the seismic hazard by increasing the down-dip limit of the seismogenic zone and extending the rupture zone inland near population centers.

Geodetic inversions of major slow slip events (SSEs) in northwest Washington from 1997-2008 reveal that only 50-60% of the long-term strain accumulation is released [Chapman and Melbourne, 2009; Schmidt and Gao, 2010]. Smaller SSEs, which are difficult to resolve geodetically, may account for the remaining slip deficit. Based on the tremor that accompanies the slow slip, Wech *et al.* (2009) inferred that up to 45% of the strain budget might be attributed to background activity in the inter-ETS interval. This would suggest that nearly the entire strain budget that is accumulated at ~ 35 km depth on the plate interface is released in ETS activity. In contrast, rate-and-state simulations of SSEs have predicted that a sizable portion of the slip deficit remains after several events, which may be due to dilatant strengthening during SSEs [Segall *et al.* 2010].

Early investigations of campaign GPS observations and leveling data identified a double-locked zone in Cascadia, with the second locked zone being located at 30 to 40 km depth [Verdonck, 2005; McCaffrey *et al.*, 2000]. Recent analysis of continuous GPS data in Cascadia identified a secondary locked zone coincident with the slow slip zone where up to $\sim 30\%$ coupling during the inter-ETS period [Holtkamp and Brudzinski, 2010]. Chapman and Melbourne (2009) reported long-term locking below 25 km depth of up to $\sim 15\%$ when using GPS derived solutions of repeated ETS events in northern Washington to constrain the downdip limit of the transition zone. Although these

analyses allow for up to 30% secondary locking, the relatively large uncertainties in the GPS data have made constraining the amount of secondary locking difficult.

The kinematic behavior of ETS has predominately been characterized using geodetic (i.e. GPS) and seismic measurements from the last 1-2 decades. Historical leveling and tide gauge data, which extend back nearly 8 decades, provide a means to supplement and extend these recent observations to gain a better understanding of long-term deformation in the ETS zone. When tied to an absolute reference frame with tide gauge data, leveling data provide precise uplift measurements with uncertainties significantly lower than vertical GPS measurements. *Verdonck* [1995] was one of the first to analyze and interpret the coastal uplift pattern using historical leveling data. *Burgette et al.* [2009] refined this data set, and modeled it to infer the distribution of interseismic locking on the plate interface. When the interseismic locking signal is removed from the leveling data, *Burgette et al.* [2009] identified an uplift signature that tracks along the eastern edge of the coast range. This residual uplift does not correlate with elevated topography, indicating that the strain associated with the uplift must be released over the megathrust earthquake cycle. This uplift signature cannot readily be resolved with locked zone models that prescribe a slip rate deficit that decreases monotonically with depth, as is typically done. We use historical leveling and GPS profiles along the Cascadian subduction zone to investigate the maximum allowable strain accumulation in, or near, the ETS zone that is not completely released during slow slip events. Our findings suggest that up to 20% of the strain may be stored over multiple ETS cycles.

Methodology

For this study, the vertical displacements of four east-west leveling profiles along Cascadia are analyzed: three in Oregon, and one in northern Washington (Figure 1). Relative uplift rates are derived from first- and second-order leveling surveys along highways in western Oregon and Washington. The National Geodetic Survey (NGS) performed the first leveling survey for most of the profiles beginning in the early 1930s, with additional leveling campaigns in the early 1940s and the late 1980s. Recently, *Burgette et al.* [2009] improved upon the NGS data set by making secondary ties to benchmarks, correcting for sea level rise rates, and improving the data processing. This dataset provides approximately 80 years worth of geodetic uplift rates along Cascadia, a significantly longer time span than observations made with GPS measurements. Each leveling profile is tied to benchmarks at tide gauge stations. After accounting for regional sea level rise, the tide gauge uplift rates are used to provide an absolute reference frame to the relative uplift rates from the leveling profiles. This, along with additional processing methods, helps to significantly reduce the standard error of benchmark uplift rates to $\sim 0.2 \text{ mm a}^{-1} - 0.5 \text{ mm a}^{-1}$, with the error increasing and propagating from west to east away from the tide gauge benchmarks. Refer to *Burgette et al.* [2009] for the complete details of the processing procedure.

To model the subduction zone, a backslip method is used to estimate the slip deficit on the subduction interface [*Savage et al.*, 2000]. The convergence rate is calculated using the Juan de Fuca-Oregon forearc Euler pole of *Wells and Simpson* [2001] for the Oregon profiles and the Juan de Fuca-North America pole of *Mazzotti et al.* [2003] for the Washington profile. The Juan de Fuca slab interface is modeled by discretizing the depth contours of *McCroory et al.* [2004] into triangular subfault patches.

Surface deformation is estimated using elastic Green's functions calculated from the boundary element program Poly3D [Thomas, 1993]. Slip is ascribed using a combination of dip-slip and strike-slip motion to account for oblique convergence of the Juan de Fuca plate with North America. The slip deficit along the plate interface is prescribed by four free parameters: the down-dip extent of the primary seismogenic zone (locked zone), the down-dip extent of the transition zone, and a zone of partial coupling near the ETS zone where the location and magnitude of the coupling are allowed to vary.

The slip deficit rate in the seismogenically locked zone is assumed to be the full convergence rate and fully locked to the trench. In the transition zone, the slip deficit decays exponentially from the full convergence rate to zero as described by Wang *et al.* [2003]. The slip deficit near the ETS zone is prescribed by a zone of partial coupling that follows the shape of a Gaussian with a 1-sigma along-dip width of 2 km. The magnitude of coupling and the location of the peak of the Gaussian are allowed to vary. This distribution of strain accumulation was chosen to correspond with the general shape of observed tremor density. Although the coupling distribution may differ with the distribution of tremor, our model results are relatively insensitive to the prescribed shape so long as the depth and magnitude of the coupling distribution are similar. An iterative procedure is run to explore the full model parameter space. Model results including and excluding coupling in the ETS zone are compared to the observed displacements and a weighted root mean square (WRMS) values are used to evaluate the goodness of fit (Table 1).

Results

Northern Washington Leveling Profile

The modeled fits prefer a peak coupling of 5-15% located at 33-38 km depth. The eastern side of the northern Washington leveling profile has a gap where it crosses the Puget Sound. The points directly west of the Puget Sound gap (longitude of ~-123W) show a leveling off of uplift rates, which diverges from the linear trend in decreasing uplift rates observed in the western portion of the profile. A model that includes coupling in the ETS zone better fits these points on the western edge of Puget Sound, but the lack of data within the Sound makes quantifying the precise magnitude of the coupling difficult.

Astoria Leveling Profile

The uplift on the eastern-end of the profile extending east from Astoria, OR is relatively distinct, but under-fit by the optimal model because of the significantly more abundant data points on the western end of the profile. We can improve the fit of the data on the eastern end of the profile by shifting the peak of the coupling in the ETS zone to 34 km depth and increasing the coupling to 20% at a cost of ~9% increase in the overall WRMS for the entire dataset. The preferred model for Astoria has a peak secondary coupling of 10-20% located at 28-34 km depth.

Newport Leveling Profile

The Newport profile is significantly better fit when coupling near the ETS zone is included. The secondary uplift is very distinct and the relatively more dense data sampling on the eastern end of the profile allows us to better constrain the coupling near the ETS zone. As can be seen in figure 2, the distance of the coastal benchmarks from the locked zone and the lack of geodetic observations nearer to the trench make it difficult to uniquely constrain the downdip edges of the locked and transition zones. This leads to some uncertainty in the amount of coupling in the primary locked zone. Decreasing the coupling in the seismogenically locked zone to 50% coupling would extend the locked zone to a depth of 13 km and would be accompanied by a similar transition zone depth of 32 km. Regardless of how coupling is ascribed in the primary locked zone, the secondary uplift signature is still best fit with a midpoint of approximately 32-35 km depth with partial coupling of 12-20%.

Bandon Leveling Profile

The Bandon profile is the only profile that is a statistically better fit with little to no coupling near the ETS zone. The best fit has a 1% coupling at 25 km, which is at the edge of the parameter space. While these parameters provide a minimal WRMS fit to the entire profile they do not fit the eastern most data very well. The eastern most extent of the Bandon profile ends in the region where the secondary uplift is observed in the other two Oregon profiles. The last few eastern points on the profile show an increasing uplift trend. Being these few points have a minimal impact on the overall fit of the profile, the optimized parameters do not adequately fit these eastern points. When a forward model is forced to fit the eastern most points, the results indicate a secondary coupling of 28-32 km depth with 5-10% coupling, although this leads to some systematic misfits of the data directly west of the secondary uplift. This procedure raises the WRMS by 10% compared to the optimal model with no coupling. The preferred fit is indicated in parentheses in Table 1. Alternatively, lowering the value of gamma to 0.1-0.2 can better fit the eastern data without adversely affecting the fit of the western data. Models using the small gamma values result in similar locked zone and secondary coupling depths, while the transition zone is significantly deeper at ~30-35 km. Although a gamma this low may not be physically plausible, it could indicate that structural heterogeneities in this area may not be adequately modeled with an elastic half-space approach.

GPS Analysis

To supplement the leveling results, a similar modeling and analysis procedure is done with horizontal GPS velocities. We use network site velocities in Cascadia from continuous GPS observations made available through UNAVCO's Plate Boundary Observatory (PBO) [<http://pbo.unavco.org/>] as well as a combination of survey and continuous GPS measurements compiled and analyzed by *McCaffrey et al.* [2007]. The velocities are restricted to sites with at least two years of data. The sites are also limited to those in western Cascadia and are spatially binned to coincide with the leveling profiles. Sites near the volcanic centers of Mt. St. Helens, Mt. Hood, Mt. Shasta, and Lassen Peak are removed. The rotation of Oregon and southern Washington is removed using the pole and rate of rotation derived by *McCaffrey et al.* [2007]. The

north and east oriented velocity vectors are rotated into convergence normal and convergence parallel components. This allows us to focus on the convergence parallel component, where the maximum deformation signal is expected to be observed.

The subtle change in the surface deformation with a locked ETS patch combined with higher uncertainties in the GPS data makes the detection of partial coupling in the ETS zone difficult. As can be seen with the Neah Bay profile in particular, a model containing a moderate ($\sim 10\text{-}15\%$) amount of coupling near the ETS zone does not provide a significantly different fit to the data (Table 2). For all the profiles, except Newport, the GPS results reveal a shallower seismogenically locked zone than the leveling results. This could, in part, be due to the fact that the GPS data are averaged over different time intervals. Time-dependent deformation along the fault since the last major rupture (i.e. viscous relaxation of the lower crust or upper mantle) could affect the GPS and leveling data differently. Being that our model assumes an isotropic elastic medium, we do not explore how the deformation might evolve with time. The Newport and Bandon profiles have especially shallow locked zones, although models that have deeper locked zones and shallower transition zones can adequately fit the data as well. The relatively short averaging interval of the GPS data, which covers a limited number of ETS cycles, might also affect the modeled long-term coupling in the ETS zone. For example, if a site velocity is derived using an averaging interval of three years and the ETS cycle is ~ 18 months the modeled results could show up to a 50% long-term strain accumulation in the ETS zone even if there is no actual long-term strain in that region. This likely explains why some GPS profiles tend to have higher coupling ratios near the ETS zone. The location of the modeled peak coupling tends to match fairly well with the leveling results, although the coupling in the Neah Bay profile is best fit a few kilometers further updip.

Discussion

Based on the prevalence of the secondary uplift signature in all of the Cascadia leveling lines and the modeled location of the secondary locking being near the ETS region, we hypothesize that the secondary locking is due to strain being accumulated in the ETS region over decadal time scales. The macroscopic relationship between SSEs and tremor activity in Cascadia has been shown to be relatively well correlated both spatially and temporally, although inferences from geodetic observations in northern Washington tend to locate slip slightly updip of the peak tremor activity [e.g. *Wang et al.*, 2008; *Wech et al.*, 2009]. When the distribution of tremor is plotted with the best-fit modeled backslip profiles of the leveling data, the peak coupling in the ETS zone is also located slightly updip of the peak tremor activity, placing the coupling near the geodetically observed slow slip (Figure 3).

As addressed by *McCaffrey et al.* [2013], it is possible that the seismogenic zone is not fully locked and is only partially coupled. The assumption that the slip deficit rate in the seismogenically locked zone equals the full convergence rate does affect the depth of the locked zone and transition zone in our results. The Astoria leveling profile can be fit reasonably well with a seismogenically locked zone with coupling down to 70%, while the Newport profile can be reasonably fit with as low as 50% coupling in the locked zone. Although the amount of coupling in the seismogenic zone affects the depths of the locked zone and transition zone, it has a relatively insignificant effect on

the coupling in the ETS zone and only shifts the model parameters by up to 1-2 km depth and 1-4% coupling. Conversely, due to updip subsidence caused by the addition of coupling near the ETS zone, models that include this coupling tend to have modeled locked zones that are slightly deeper and shifted to the east. The difference in locked zone depths is typically only 1-2 km, but considering the seismic hazard imposed by the depth of the locked zone, this may serve as an important consideration for future hazard mitigation efforts.

A possible explanation for the residual strain accumulation in the ETS region is that the combination of regular and inter-ETS SSEs are not accommodating the total slip deficit of the subducting Juan de Fuca plate. The combination of ETS and inter-ETS events may account for a significant portion of the remaining slip deficit in this region [Aguiar *et al.*, 2009]. However, inter-ETS tremor is found downdip of regular ETS tremor [Wech *et al.*, 2009, Wech and Creager, 2011] so may only accommodate the remaining slip deficit in the downdip portion of the ETS zone, while leaving a fraction of the slip deficit in the updip portion of the ETS zone.

Conclusions

Models that include up to ~20% locking along the updip edge of the ETS zone provide a better fit to the leveling profiles in Cascadia. This coupling is difficult to resolve in the GPS data, but may have a significant impact on the kinematic behaviors of the Cascadian subduction zone. Considering no topographical features exist to indicate the coupling, and associated uplift, persists across megathrust earthquake cycles, it may be that megathrust events extend into the updip portion of ETS zone, either seismically or post-seismically, releasing the accumulated strain and affectively extending the rupture area further down-dip than previous models predict. Alternatively, the accumulated strain could be released through aseismic processes, such as in a future ETS event or as afterslip.

References

- Aguiar, A. C., T. I. Melbourne, and C. W. Scrivner (2009), Moment release rate of Cascadia tremor constrained by GPS, *J. Geophys. Res.*, 114, B00A05, doi:10.1029/2008JB005909.
- Chapman, J. S. and T. I. Melbourne (2009), Future Cascadia megathrust rupture delineated by episodic tremor and slip, *Geophys. Res. Lett.*, 36, L22301, doi:10.1029/2009GL040465.
- Dragert, H., K. Wang, and T. S. James (2001), A silent slip event on the deeper Cascadia subduction interface, *Science*, 292, 1525-1528, DOI: 10.1126/science.1060152.
- Burgette, R. J., R. J. Weldon, II, and D. A. Schmidt (2009), Interseismic uplift rates for western Oregon and along-strike variation in locking on the Cascadia subduction zone, *J. Geophys. Res.*, 114, B01408, doi:10.1029/2008JB005679.
- Holtkamp, S. and M. R. Brudzinski (2010), Determination of slow slip episodes and strain accumulation along the Cascadia margin, *J. Geophys. Res.*, 115, B00A17, doi:10.1029/2008JB006058.
- McCaffrey, R., R. W. King, S. J. Payne, and M. Lancaster (2013), Active tectonics of northwestern U.S. inferred from GPS-derived surface velocities, *J. Geophys. Res. Solid Earth*, 118, 709–723, doi:10.1029/2012JB009473.

- McCaffrey, R., A. I. Qamar, R. W. King, R. Wells, G. Khazaradze, C. A. Williams, C. W. Stevens, J. J. Vollick, and P. C. Zwick (2007), Fault locking, Block Rotation and Crustal Deformation in the Pacific Northwest, *Geophysical Journal International*, v. 169, p. 1315-1340, doi:10.1111/j.1365-246X.2007.03371.x
- McCaffrey, R., M. D. Long, C. Goldfinger, P. Zwick, J. Nabelek, and C. Smith (2000), Rotation and plate locking at the southern Cascadia subduction zone, *Geophysical Research Letters*, 27, 3117-3120.
- McCrory, P. A., J. L. Blair, D. H. Oppenheimer, and S. R. Walter (2004), Depth to the Juan de Fuca slab beneath the Cascadia subduction margin: A 3-D model for sorting earthquakes, *U. S. Geol. Surv. Data Ser. DS-91*, 1 CD-ROM.
- Rogers, R., and H. Dragert (2003), Episodic Tremor and Slip on the Cascadia Subduction Zone: The Chatter of Silent Slip, *Science*, 300, 1942-1943, DOI: 10.1126/science.1084783.
- Savage, J. C, Svarc, J.L., Prescott, W. H., Murray, M. H., 2000, Deformation across the forearc of the Cascadia subduction zone at Cape Blanco, Oregon, *J. Geophys. Res.*, v. 105 p. 3095-3102.
- Schmidt, D. A. and H. Gao (2010), Source parameters and time-dependent slip distributions of slow slip events on the Cascadia subduction zone from 1998 to 2008, *J. Geophys. Res.*, 115, B00A18, doi:10.1029/2008JB006045.
- Segall, P., A. M. Rubin, A. M. Bradley, and J. R. Rice (2010), Dilatant strengthening as a mechanism for slow slip events. *J. Geophys. Res.*, 115, B12305, doi:10.1029/2010JB007449.
- Thomas, A.L. (1993), Poly3D: A Three-Dimensional, Polygonal Element, Displacement Discontinuity Boundary Element Computer Program with Applications to Fractures, Faults, and Cavities in the Earth's Crust : M.S. Thesis, Stanford University, CA.
- Verdonck, D. (2005), An inverse dislocation model of surface deformation in western Washington, *Tectonophysics*, 395(3-4), 179-191, doi:10.1016/j.tecto.2004.09.010.
- Verdonck, D. (1995), 3-Dimensional model of vertical deformation at the southern Cascadia subduction zone, western United States, *Geology*, 23(3), 261-264, doi:10.1130/0091-7613.
- Wang, K. Wells, R., Mazzotti, S., Hyndmann, R. D., and T. Sagiya (2003), A revised dislocation model of interseismic deformation of the Cascadia subduction zone, *J. Geophys. Res.*, 108.
- Wang, K., H. Dragert, H. Kao, and E. Roeloffs (2008), Characterizing an "uncharacteristic" ETS event in northern Cascadia, *Geophys. Res. Lett.* 35, L15303, doi:10.1029/2008GL034415.
- Wech, A. G. and K. C. Creager, 2011, A continuum of stress, strength and slip in the Cascadia transition zone, *Nature GeoSci.*, 4, 1-5, doi:10.1038/ngeo121.
- Wech, A. G., K. C. Creager, and T. I. Melbourne (2009), Seismic and geodetic constraints on Cascadia slow slip, *J. Geophys. Res.*, 114, B10316, doi:10.1029/2008JB006090.
- Wells, R. E., and Simpson, R. W., 2001, Microplate motion of the Cascadia forearc and implications for subduction deformation; *Earth Planets Space*, v. 53, p. 275-283.

Table 1. Comparison of optimal model fits of the leveling data with and without including coupling near the ETS zone. The Bandon profile also includes the preferred fit results in parentheses. Statistical significance is calculated using an F-test.

* Results are at the edge of the modeled parameter space.

Leveling Results	Neah Bay	Astoria	Newport	Bandon
No Locking in ETS zone				
Locked zone depth (km)	16	17	5*	10.5
Transition zone depth (km)	35.5	27	27	18
WRMS (mm/yr)	0.5539	0.9492	0.6596	0.5631
Including Locking in ETS zone				
Locked zone depth (km)	17	19	7	10.5 (10.5)
Transition zone depth (km)	36	24	31	18 (18.5)
Peak ETS zone coupling (%)	10	11	15	1 (8)
Midpoint of ETS zone locking (units?)	35.5	28	32.5	25* (29.5)
WRMS (mm/yr)	0.4455	0.8884	0.4525	0.5612 (0.6165)
Statistically Significant (90%)	Yes	No	Yes	No (n/a)
Statistically Significant (70%)	Yes	Yes	Yes	No (n/a)

Table 2. Comparison of model fits of the leveling data with and without including coupling near the ETS zone. Statistical significance is calculated using an f-test.

* Results are at the edge of the modeled parameter space.

GPS Results	Neah Bay	Astoria	Newport	Bandon
No Locking in ETS zone				
Locked zone depth (km)	15	12	5*	5*
Transition zone depth (km)	31	24	42	30
WRMS (mm/yr)	1.5274	3.0148	1.3661	1.8831
Including Locking in ETS zone				
Locked zone depth (km)	16	11	9	5*
Transition zone depth (km)	27	24	31	27
Peak ETS zone coupling (%)	12	11	28	40*
Midpoint of ETS zone locking	29	28	32	29
WRMS (mm/yr)	1.5113	3.1435	1.3235	1.4994
Statistically Significant (90%)	No	No	No	Yes
Statistically Significant (70%)	No	No	No	Yes

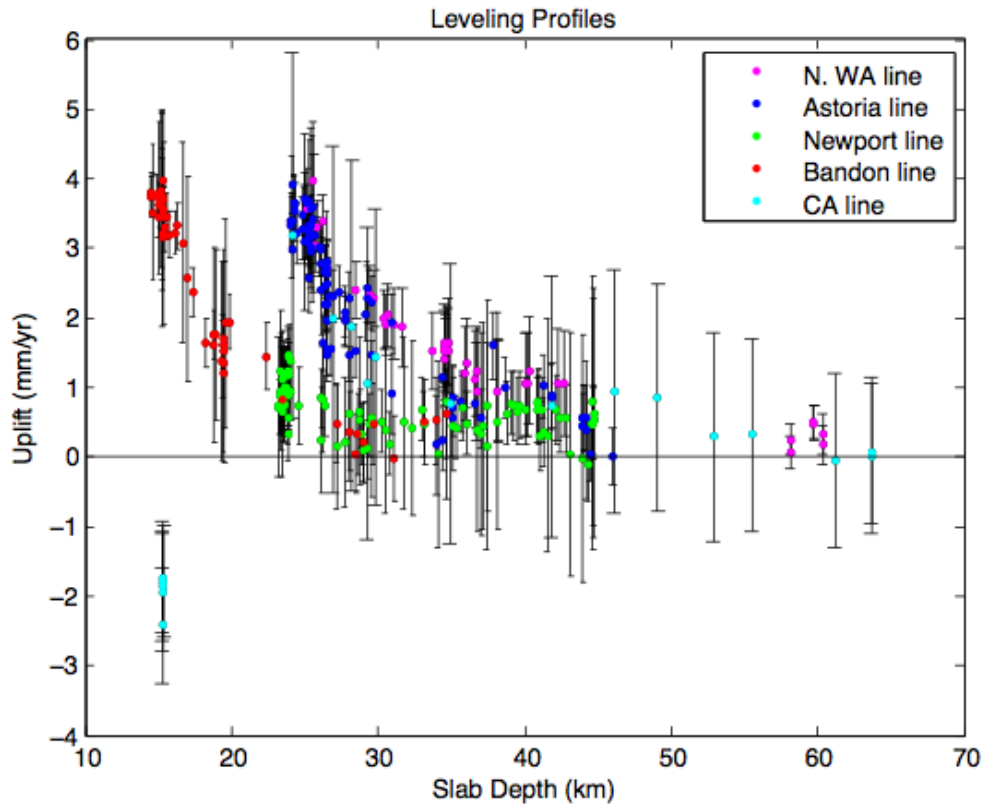


Figure 1: The leveling profiles for each east-west line consider in this study. Several profiles show a subtle rise in uplift above the 40km slab-depth contour.

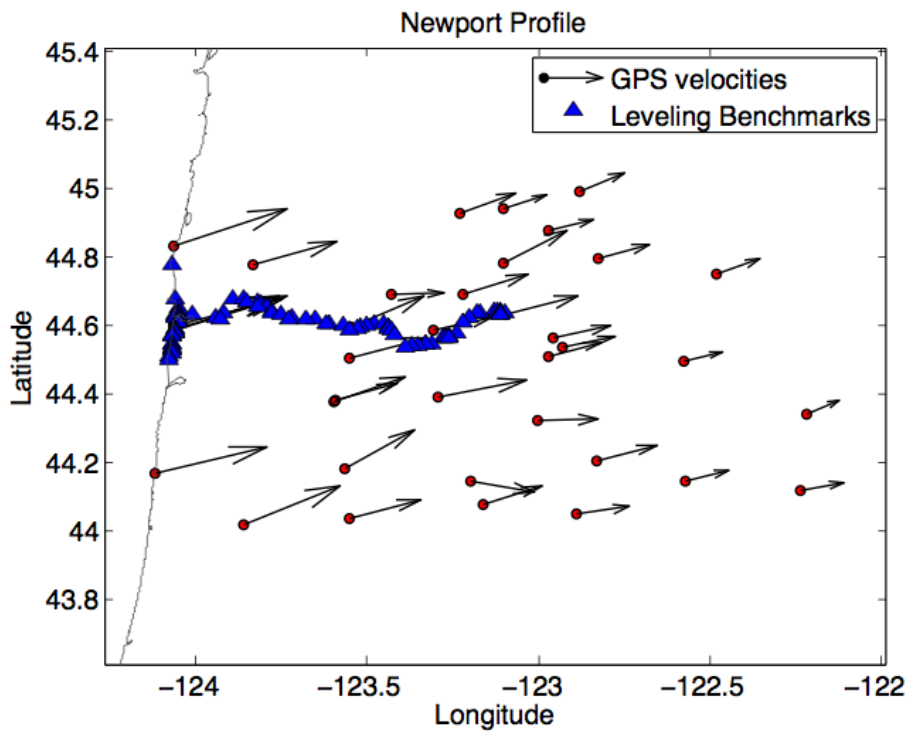
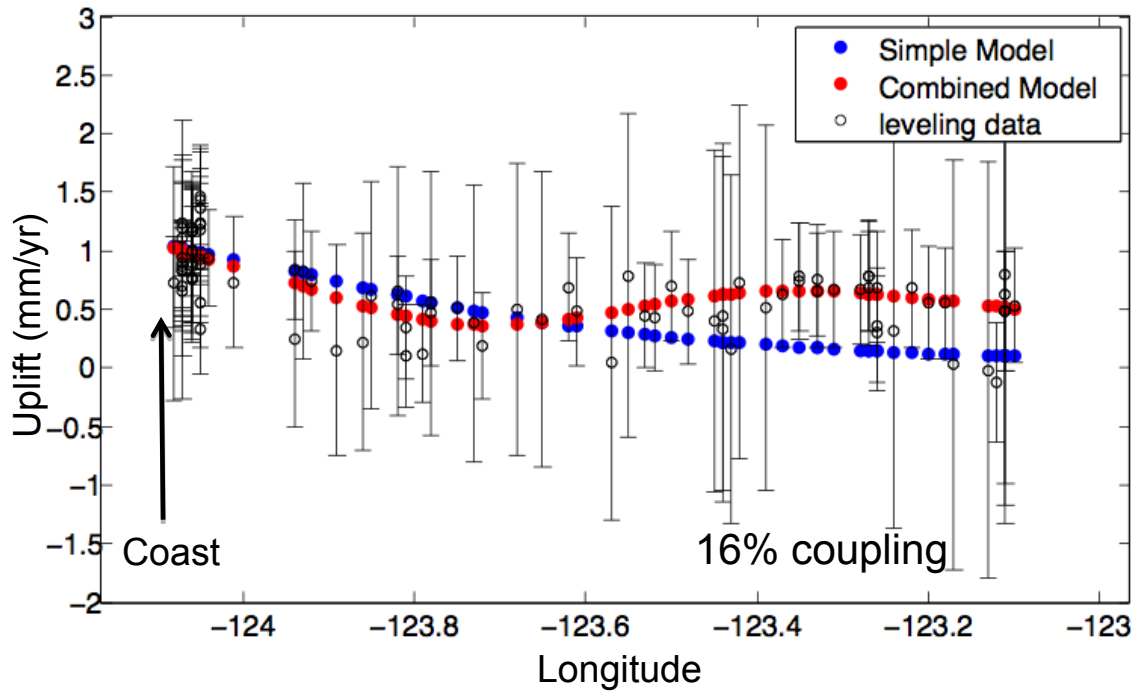


Figure 2. The Leveling data (top) and GPS velocities (bottom) for Newport, OR. The leveling data are best fit with $\sim 16\%$ coupling in the ETS zone (red dots on top plot).

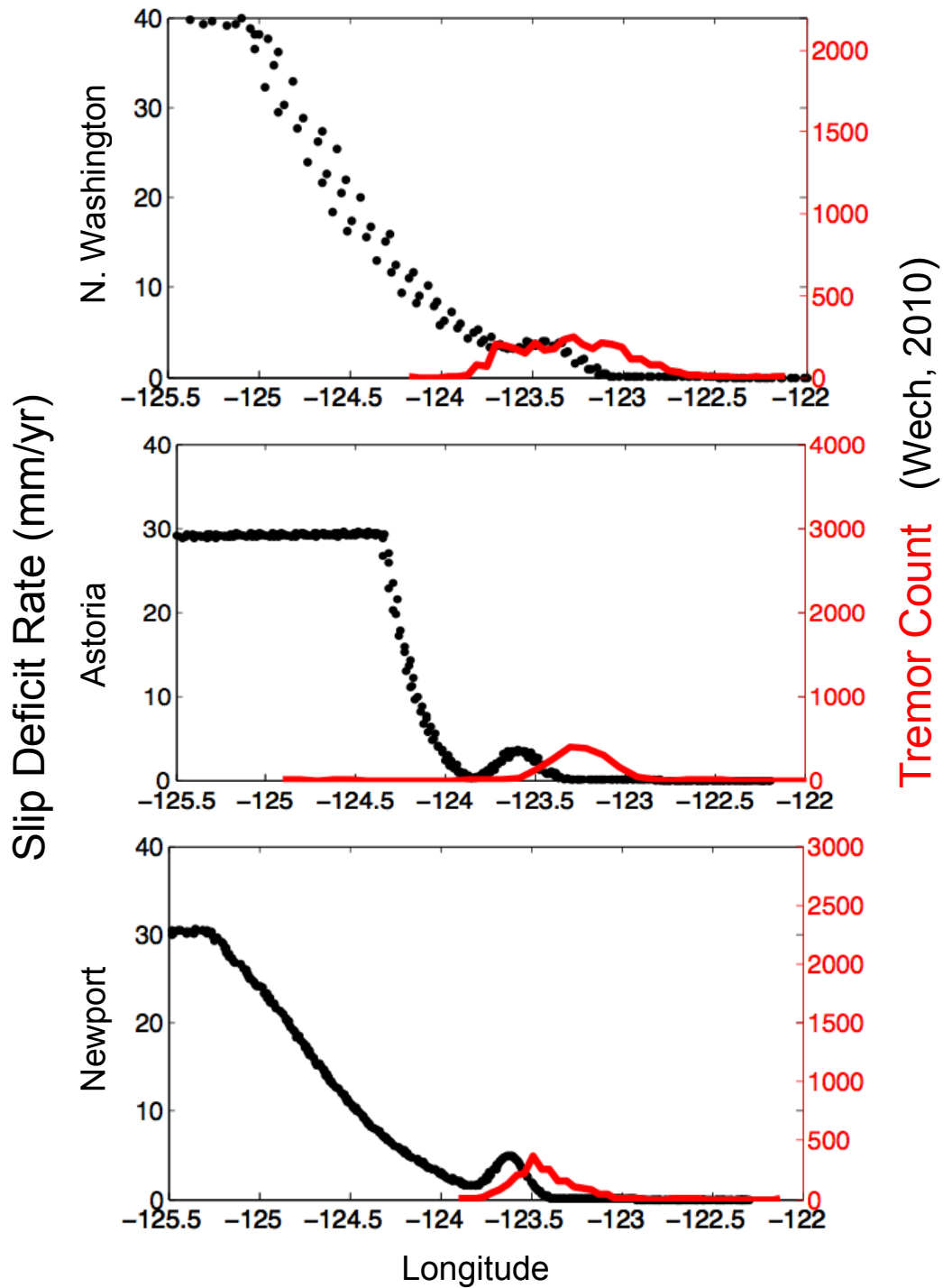


Figure 3. The best-fit slip-deficit rate functions (black dots) along the plate interface feature a locked zone on the west end, a decay of slip rate in the transition zone, and secondary increase in slip-deficit rate in the ETS zone. This secondary zone of strain accumulation overlaps with the location of tremor (red dots).